Separating viscoelasticity and poroelasticity of gels with different length and time scales

Qi-Ming Wang · Anirudh C. Mohan · Michelle L. Oyen · Xuan-He Zhao

Abstract Viscoelasticity and poroelasticity commonly co-exist as time-dependent behaviors in polymer gels. Engineering applications often require knowledge of both behaviors separated; however, few methods exist to decouple viscoelastic and poroelastic properties of gels. We propose a method capable of separating viscoelasticity and poroelasticity of gels in various mechanical tests. The viscoelastic characteristic time and the poroelastic diffusivity of a gel define an intrinsic material length scale of the gel. The experimental setup gives a sample length scale, over which the solvent migrates in the gel. By setting the sample length to be much larger or smaller than the material length, the viscoelasticity and poroelasticity of the gel will dominate at different time scales in a test. Therefore, the viscoelastic and poroelastic properties of the gel can be probed separately at different time scales of the test. We further validate the method by finite-element models and stress-relaxation experiments.

Keywords Poroviscoelasticity · Hydrogel · Tissue · Stress-relaxation test · Indentation

1 Introduction

A cross-linked polymer network can imbibe solvent molecules to form a gel. Gels are major constituents of plant and animal tissues [1–4], and widely used in diverse applications including drug delivery [5], tissue engineering [6, 7], soft machines [8–10], microfluidics [11, 12], oilfields [13],

Q.-M. Wang · A. C. Mohan · X.-H. Zhao (✉)
Soft Active Materials Laboratory,
Department of Mechanical Engineering and Materials Science,
Duke University, Durham, NC 27708, USA
e-mail: xz69@duke.edu

M. L. Oyen
Cambridge University Engineering Department,
Trumpington St., CB2 1PZ Cambridge, UK

and food processing [14]. Mechanical properties of gels are of critical importance to the well-being of tissues and various applications of gels. The mechanical behaviors of gels are generally time-dependent. Solvent migration in a gel gives poroelasticity of the gel [15–23], while rearrangements of polymer chains and reversible crosslinks contribute to viscoelasticity of the gel [24–26]. Many methods, such as parallel-plate compression test and indentation test, have been used to probe either poroelastic or viscoelastic property of gels, while assuming the other property is negligible [16, 24–29]. However, the viscoelasticity and poroelasticity usually coexist in gels, leading to complex time-dependent behaviors [30–34]. As a result, measuring both poroelastic and viscoelastic parameters of a gel is still a challenging task in physics and mechanics [34–50]. While many theories for coupled viscoelasticity and poroelasticity of polymer gels have been developed [51–57], only very few experimental methods have been proposed to distinguish viscoelastic and poroelastic properties of polymer gels [31, 32].

Here, we report a method capable of separating viscoelasticity and poroelasticity of a gel such that they manifest themselves at different time scales in mechanical tests. The basic idea of the method can be qualitatively understood as follows. Viscoelastic characteristic time and poroelastic diffusivity of a gel define an intrinsic material length scale of the gel. On the other hand, the experimental setup for testing the gel gives a sample length scale, over which the solvent migrates in the gel. By setting the sample length to be much larger or smaller than the material length, the viscoelasticity and poroelasticity of the gel will dominate at different time scales in a test. Therefore, the viscoelastic and poroelastic properties of the gel can be probed separately at different time scales of the test.

The paper is organized as follows: In Sect. 2, we formulate a theory for ideal linear poroviscoelastic gels, and then present a general method to separate viscoelastic and poroelastic properties of gels. To validate the method, a finite-

element model is developed for parallel-plate compression tests of ideal poroviscoelastic gels in Sect. 3 of the paper. In Sect. 4, parallel-plate stress-relaxation experiments are carried out on a polyacrylamide-alginate interpenetrating hydrogel to obtain viscoelastic and poroelastic parameters of the hydrogel. Conclusive remarks are summarized in Sect. 5.

2 Theory

2.1 A theory of ideal linear poroviscoelastic gel

A theory of ideal linear poroviscoelastic gel is presented in this section. The theory is developed based on the theory of linear poroviscoelasticity by Biot [53] and the nonlinear field theories of hydrogels [51, 52]. Let us consider a poroviscoelastic gel in a homogenous state, subjected to no mechanical load, as the reference state. At the reference state, we denote C_0 as number of solvent molecules per unit volume of the gel. When the gel deforms, the displacement is a time-dependent field, u_i (x_1, x_2, x_3, t), and the linear theory gives the strain in the gel as

$$\varepsilon_{ij} = \frac{1}{2}\left(\frac{\partial u_i}{\partial x_j} + \frac{\partial u_j}{\partial x_i}\right). \tag{1}$$

Denote ε and e_{ij} to be the volumetric dilation and the deviatoric components of the strain tensor, i.e.,

$$\varepsilon = \varepsilon_{kk}, \quad e_{ij} = \varepsilon_{ij} - \frac{1}{3}\varepsilon\delta_{ij}. \tag{2}$$

The conservation of solvent molecules requires that

$$\frac{\partial C}{\partial t} + \frac{\partial J_k}{\partial x_k} = 0, \tag{3}$$

where C is the number of solvent molecules at current state per unit volume of the gel at reference state, and J_k the flux of the solvent.

Individual polymer chains and solvent molecules are commonly assumed to be incompressible. Consequently, the increase in the volume of the gel is entirely due to the additional solvent molecules absorbed, namely

$$\varepsilon_{kk} = \Omega(C - C_0), \tag{4}$$

where Ω is the volume per solvent molecule.

The free energy per unit volume of the gel at the reference state is

$$w = w\left(\varepsilon, e_{ij}, C, \varepsilon^{v,1}, \varepsilon^{v,2}, \varepsilon^{v,3}, \cdots, e_{ij}^{v,1}, e_{ij}^{v,2}, e_{ij}^{v,3}, \cdots\right), \tag{5}$$

where $\varepsilon^{v,n}$ and $e_{ij}^{v,n}$ are internal variables that characterize the viscoelastic properties of the gel.

Denote σ and s_{ij} to be the hydrostatic and deviatoric components of the stress tensor σ_{ij}, i.e.,

$$\sigma = \frac{1}{3}\sigma_{kk}, \quad s_{ij} = \sigma_{ij} - \sigma\delta_{ij}. \tag{6}$$

The equations of state of the gel have

$$\sigma = \frac{\partial w}{\partial \varepsilon}, \tag{7a}$$

$$s_{ij} = \frac{\partial w}{\partial e_{ij}}, \tag{7b}$$

$$\mu - \mu_0 = \frac{\partial w}{\partial C}, \tag{7c}$$

$$\dot{\varepsilon}^{v,n} = -\frac{1}{\eta_K^n}\frac{\partial w}{\partial \varepsilon^{v,n}}, \tag{7d}$$

$$\dot{e}_{ij}^{v,n} = -\frac{1}{2\eta_G^n}\frac{\partial w}{\partial e_{ij}^{v,n}}, \tag{7e}$$

where η_K^n is the viscosity of the n-th volumetric viscous component (Fig. 1a), η_G^n is the viscosity of the n-th deviatoric viscous component (Fig. 1b), μ is chemical potential of the solvent in the gel, and μ_0 is chemical potential of the solvent in the environment.

Considering Fig. 1, the free energy function for linear poroviscoelastic gel can be expressed as

$$w = G_R e_{ij}^2 + \frac{1}{2}K_R\varepsilon^2 + \sum_n G_n\left(e_{ij} - e_{ij}^{v,n}\right)^2$$

$$+ \frac{1}{2}\sum_n K_n(\varepsilon - \varepsilon^{v,n})^2 + \Pi[\Omega(C - C_0) - \varepsilon], \tag{8}$$

where G_R is the relaxed shear modulus, G_n is the shear modulus of the n-th shear component, K_R is the relaxed bulk modulus, K_n is the bulk modulus of the n-th bulk component, and Π is a Lagrange multiplier that imposes Eq. (4).
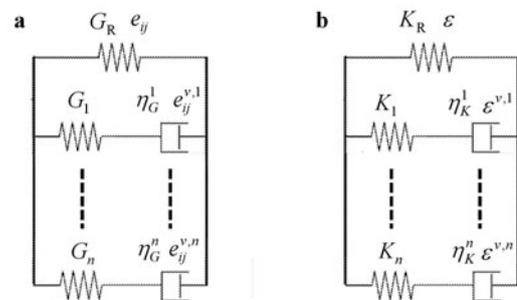
Fig. 1 Schematics for the deviatoric and volumetric components of the poroviscoelastic gel. **a** Deviatoric component; **b** Volumetric component

Therefore, from Eq. (7) we can obtain the explicit form of the equations of state

$$\sigma = K_R\varepsilon + \sum_n K_n(\varepsilon - \varepsilon^{v,n}) - \Pi, \tag{9a}$$

$$s_{ij} = 2G_R e_{ij} + 2\sum_n G_n\left(e_{ij} - e_{ij}^{v,n}\right), \tag{9b}$$

$$\mu - \mu_0 = \Omega\Pi, \tag{9c}$$

$$\dot{\varepsilon}^{v,n} = \frac{K_n}{\eta_K^n}(\varepsilon - \varepsilon^{v,n}), \tag{9d}$$

$$\dot{e}_{ij}^{v,n} = \frac{G_n}{\eta_G^n}\left(e_{ij} - e_{ij}^{v,n}\right). \tag{9e}$$

By substituting Eqs. (9b) and (9c) into (9a) and denoting $\tau_K^n = \eta_K^n / K_n$ and $\tau_G^n = \eta_G^n / G_n$, we have

$$\sigma_{ij} = 2G_{\mathrm{R}} e_{ij} + K_{\mathrm{R}} \varepsilon + 2\sum_n G_n \left(e_{ij} - e_{ij}^{v,n} \right)$$

$$+ \sum_n K_n (\varepsilon - \varepsilon^{v,n}) - \frac{\mu - \mu_0}{\Omega} \delta_{ij}, \tag{10a}$$

$$\dot{\varepsilon}^{v,n} = \frac{1}{\tau_K^n} (\varepsilon - \varepsilon^{v,n}), \tag{10b}$$

$$\dot{e}_{ij}^{v,n} = \frac{1}{\tau_G^n} \left(e_{ij} - e_{ij}^{v,n} \right), \tag{10c}$$

where τ_K^n is the characteristic time of the n-th volumetric viscous component, and τ_G^n is the characteristic time of the n-th deviatoric viscous component.

Subject to a step increase in ε and e_{ij}, the time evolution of $\varepsilon^{v,n}$ and $e_{ij}^{v,n}$ can be calculated from Eqs. (10b) and (10c) as

$$\varepsilon^{v,n} = \varepsilon \left[1 - \exp\left(-t/\tau_K^n\right) \right], \tag{11a}$$

$$e_{ij}^{v,n} = e_{ij} \left[1 - \exp\left(-t/\tau_G^n\right) \right]. \tag{11b}$$

By substituting Eqs. (11a) and (11b) into Eq. (10a), we have

$$\sigma_{ij} = 2 \left[G_{\mathrm{R}} + \sum_n G_n \exp\left(-t/\tau_G^n\right) \right] e_{ij}$$

$$+ \left[K_{\mathrm{R}} + \sum_n K_n \exp\left(-t/\tau_K^n\right) \right] \varepsilon - \frac{\mu - \mu_0}{\Omega} \delta_{ij}. \tag{12}$$

We can define the unrelaxed shear modulus $G_{\mathrm{U}} = G_{\mathrm{R}} + \sum_n G_n$, and the unrelaxed bulk modulus $K_{\mathrm{U}} = K_{\mathrm{R}} + \sum_n K_n$.

For an ideal linear poroviscoelastic gel, we assume

$$\frac{G_n}{K_n} = \frac{G_{\mathrm{R}}}{K_{\mathrm{R}}} = \frac{3(1 - 2v)}{2(1 + v)}, \tag{13a}$$

and

$$\tau_n = \tau_G^n = \tau_K^n, \tag{13b}$$

where v is the effective Poisson's ratio of the gel [16, 43, 52], and τ_n is the characteristic time of the n-th viscous component.

By substituting Eqs. (13a) and (13b) into Eq. (12), we have

$$\sigma_{ij} = 2 \left[G_{\mathrm{R}} + \sum_n G_n \exp\left(-\frac{t}{\tau_n}\right) \right] \left(\varepsilon_{ij} + \frac{v}{1 - 2v} \varepsilon_{kk} \delta_{ij} \right)$$

$$- \frac{\mu - \mu_0}{\Omega} \delta_{ij}. \tag{14}$$

Equation (14) can be further expressed in terms of Prony Series, i.e.,

$$\sigma_{ij} = 2G_{\mathrm{U}} \left\{ 1 - \sum_n g_n \left[1 - \exp\left(-\frac{t}{\tau_n}\right) \right] \right\} \left(\varepsilon_{ij} + \frac{v}{1 - 2v} \varepsilon_{kk} \delta_{ij} \right)$$

$$- \frac{\mu - \mu_0}{\Omega} \delta_{ij}, \tag{15}$$

where $g_n = G_n / G_{\mathrm{U}}$ is the coefficient of the n-th term of the Prony series.

The gradient of the chemical potential drives the flux of the solvent according to Darcy's law

$$J_i = -\left(\frac{k}{\eta \Omega^2} \right) \frac{\partial \mu}{\partial x_i}, \tag{16}$$

where η is viscosity of the solvent, and k is the permeability of the gel.

A combination of Eqs. (3), (15), and (16) gives

$$\frac{\partial C}{\partial t} = D \nabla^2 C, \tag{17}$$

where the effective diffusivity of the solvent in the gel

$$D = G_{\mathrm{U}} \left\{ 1 - \sum_n g_n \left[1 - \exp\left(-\frac{t}{\tau_n}\right) \right] \right\} \frac{2(1 - v)k}{(1 - 2v)\eta}. \tag{18}$$

From Eq. (18), the diffusivities of the gel at viscoelastically unrelaxed and relaxed states are D_{U} and D_{R}, respectively

$$D_{\mathrm{U}} = [2(1 - v)/(1 - 2v)] G_{\mathrm{U}} k/\eta, \tag{19a}$$

$$D_{\mathrm{R}} = [2(1 - v)/(1 - 2v)] G_{\mathrm{R}} k/\eta. \tag{19b}$$

Therefore, a set of material parameters that characterize an ideal poroviscoelastic gel are G_{U}, g_n, τ_n, v, and D_{U} (or D_{R}). For further simplification, if we assume there is only one dominant viscoelastic component in the gel, Eq. (15) can be expressed as

$$\sigma_{ij} = 2 \left[G_{\mathrm{R}} + (G_{\mathrm{U}} - G_{\mathrm{R}}) \exp\left(-\frac{t}{\tau}\right) \right] \left(\varepsilon_{ij} + \frac{v}{1 - 2v} \varepsilon_{kk} \delta_{ij} \right)$$

$$- \frac{\mu - \mu_0}{\Omega} \delta_{ij}. \tag{20}$$

In this simplified case, the set of material parameters are G_{U}, G_{R}, τ, v, and D_{U} (or D_{R}).

2.2 Separation of length and time scales

Based on the above theory, we propose a method to distinguish poroelastic and viscoelastic properties of a gel in a single test by separating the length and time scales of the two properties. We will illustrate the method with a simple stress-relaxation test. A gel disk immersed in a solvent is compressed by a pair of rigid impermeable parallel plates and held at a constant strain as illustrated on Fig. 2a. The reactive force F is recorded as a function of time t. It is evident that F scales with a^2, where a is the radius of the gel disk.

Let us first consider a linear poroelastic gel. After the gel disk is compressed, the reactive force decreases with time due to poroelastic stress relaxation (Fig. 2b). Because the poroelastic stress relaxation is induced by migration of solvent molecules across the radius of the gel disk into the external solvent, the time for the poroelastic relaxation scales with a^2/D [17, 21, 22, 25, 43]. Therefore, the curve of F/a^2 vs. t depends on the sample size a, such that the larger the sample the slower the relaxation (Fig. 2b). However, the curve of

F/a^2 vs. t/a^2 is independent of a, due to the a^2/D scaling of the relaxation time (Fig. 2c) [25].

We next consider a linear viscoelastic elastomer. The viscoelastic stress relaxation is caused by local rearrangements of polymer chains and/or crosslinks, and thus independent of the sample size. Therefore, the curve of F/a^2 vs. t is independent of a (Fig. 1d), but the curve of F/a^2 vs. t/a^2 depends on a (Fig. 2e).
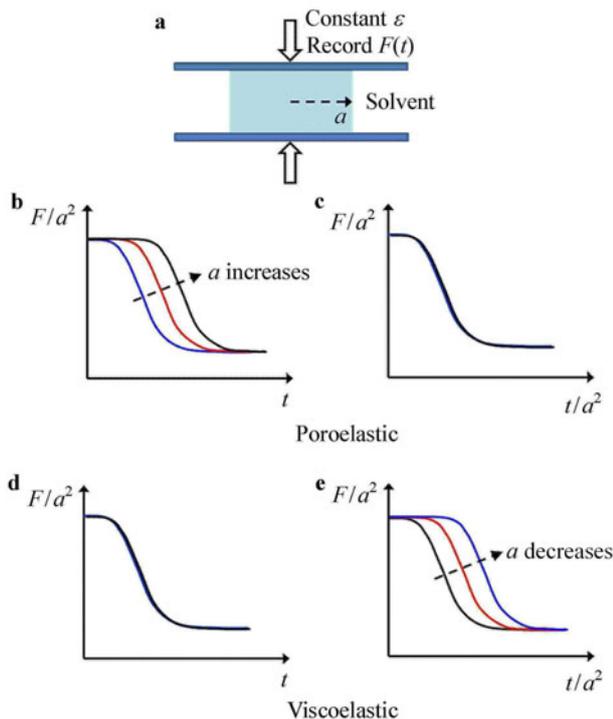
Fig. 2 a A disk is under parallel-plate stress-relaxation test; **b** If the material is poroelastic, the curve of F/a^2 vs. t depends on the radius of the disk a; **c** But the curve of F/a^2 vs. t/a^2 is independent of a; **d** On the other hand, if the material is viscoelastic, the curve of F/a^2 vs. t is independent of a; **e** But the curve of F/a^2 vs. t/a^2 depends on a

Now, let us study a gel with both viscoelastic and poroelastic properties. The viscoelastic characteristic times for the gel are in a range, i.e., $\tau_{min} \leqslant \tau_1 < \tau_2 < \tau_n \leqslant \tau_{max}$. The effective diffusivity of the solvent in the gel is D_U at viscoelastically unrelaxed state and D_R at viscoelastically relaxed state. The viscoelastic characteristic times and the poroelastic diffusivities can define intrinsic material length scales of the poroviscoelastic gel as [25]

$$\Lambda_U = \sqrt{D_U \tau_{min}}, \quad \Lambda_R = \sqrt{D_R \tau_{max}}, \tag{21}$$

where Λ_U is the unrelaxed material length and Λ_R the relaxed material length of the gel. On the other hand, the experimental setup can give a sample length scale a (e.g. the radius of the gel disks), over which the solvent transports in the gel sample during the tests (Fig. 2a).

We propose that the viscoelasticity and poroelasticity of a gel can be measured at different time scales of a test, by choosing sample lengths to be much larger or smaller than the material lengths as illustrated on Fig. 3. In the large-sample case (Fig. 3a), we set the sample lengths in the test to be very large, expecting that

$$a \gg \Lambda_R. \tag{22}$$

If Eq. (22) is satisfied, the time scale for poroelastic relaxation, a^2/D_R, is much larger than the largest time scale for viscoelastic relaxation, τ_{max}. In this case, the stress relaxation curves are initially sample-size independent within a relatively short period of time, $\sim \tau_{max}$, due to the dominant viscoelastic relaxation (Fig. 2a). In this period, the gel can be regarded as a viscoelastic gel at the undrained state or a viscoelastic elastomer. Following established theories, the viscoelastic properties of the gel can be obtained from this part of the curves [45]. When the force decreases below a middle-range plateau, F_m, the stress-relaxation curves become sample-size dependent, as the poroelastic relaxation becomes dominant in a relatively long time period, $\sim a^2/D_R$ (Fig. 3a). In this period, the gel can be regarded as a poroelastic material with viscoelastically relaxed modulus. The poroelastic properties of the gel can be obtained from this part of the curves [27, 43, 44].

In the small-sample case (Fig. 3b), we set the sample lengths in the test to be very small, expecting that

$$a \ll \Lambda_U. \tag{23}$$

If Eq. (23) is satisfied, the time scale for poroelastic relaxation, a^2/D_U, is much smaller than the smallest time scale for viscoelastic relaxation, τ_{min}. In the small-sample case, the stress relaxation curves are initially sample-size dependent within a relatively short time period, $\sim a^2/D_U$, due to the dominant poroelastic relaxation Fig. 3b. In this period of time, the gel can be regarded as a poroelastic material with viscoelastically unrelaxed modulus. The viscoelastic properties of the gel can be obtained from this part of the curves. When the force decreases below F_m, the stress-relaxation curves become sample-size independent, as the viscoelastic relaxation becomes dominant in a relatively long time period, $\sim \tau_{max}$. In this period, the gel can be regarded as a viscoelastic gel at the drained state. The viscoelastic properties of the gel can be obtained from this part of the curves.

3 Finite element model

To validate the above method on separating viscoelasticity and poroelasticity, we model the compressive stress-relaxation tests on an ideal poroviscoelastic gel disk with finite-element software ABAQUS [38, 43, 44]. An axisymmetric model is adopted, as shown in Fig. 2a. The gel thickness is set as 0.1 times of the radius of the gel disk. Due to symmetry, only half of the model is analyzed. The gel is assumed to be an ideal linear poroviscoelastic material with
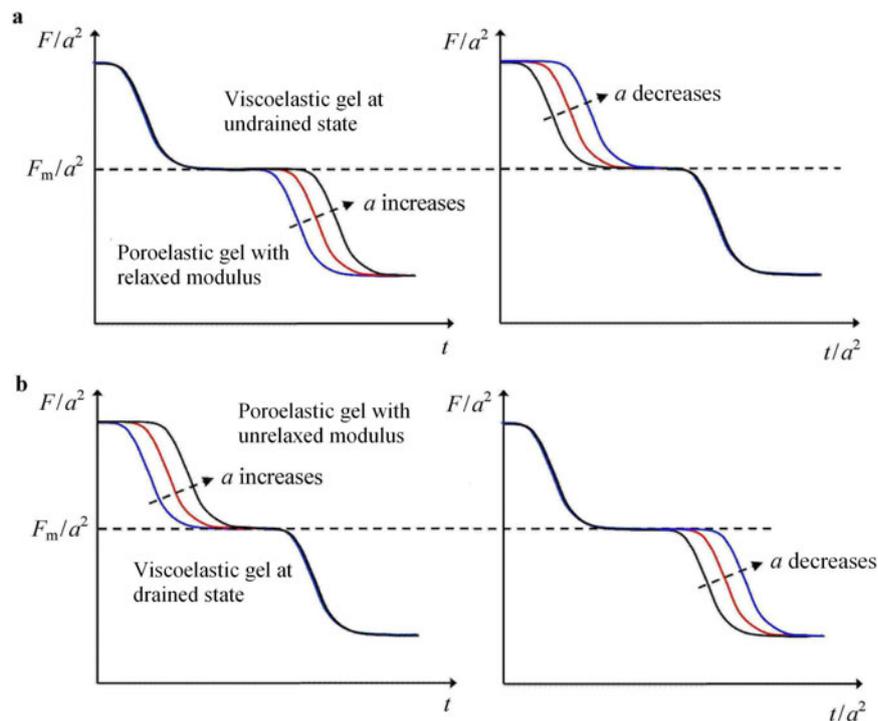
Fig. 3 Schematic curves on separating viscoelasticity and poroelasticity of a gel. **a** For the large-sample case ($a \gg \Lambda_R$), the gel is viscoelastic in the short-time period and poroelastic in the long-time period; **b** For the small-sample case ($a \ll \Lambda_U$), the gel is poroelastic in the short-time period and viscoelastic in the long-time period

five material parameters: the unrelaxed and relaxed shear moduli G_U and G_R, the effective Poisson's ratio v, the viscoelastic characteristic time τ, and the unrelaxed (or relaxed) diffusivity D_U (or D_R). In ABAQUS, the ideal linear poroviscoelastic gel is implemented as a viscoelastic and soil-type material with "pore/fluid stress" elements, CAX4P. The modulus and Poisson's ratio of the gel are taken to be $G_U/G_R = 2$ and $v = 0$. The results are further validated to be insensitive to the mesh by reducing the mesh size of the model. A step strain of 5% is instantaneously applied to the gel disk and held for a long time. The calculation is implemented as a transient consolidation analysis with zero fluid velocity. The recorded reaction forces on the impermeable plate are plotted in Fig. 4.

For the large-sample case, the normalized radii of the gel disks, a/Λ_R, are set to be 100, 200, and 300. Figure 4a shows that the viscoelasticity dominates in the short-time period, and the poroelasticity in the long-time period. For the small-sample case, the normalized radii of the gel disks, a/Λ_U, are set to be 0.707×10^{-2}, 1.41×10^{-2}, and 2.12×10^{-2}. From Fig. 4b, it is evident that the poroelasticity of the gel dominates in the short-time period, and the viscoelasticity in the long-time period.

4 Experiment

To further illustrate the capability of the method in measuring poroviscoelastic properties of gels, we carry out parallel-plate stress-relaxation tests [25] on a polyacrylamide-alginate interpenetrating hydrogel [58–61]. The hydrogel was prepared by mixing ionically cross-linked alginate and covalently cross-linked polyacrylamide (see Ref. [40] for details). Hydrogel disks with thickness of 3 mm were cut out by metal punches with radii from 3.675 to 7.95 mm. The hydrogel disks were then mounted between two smooth steel plates (radius 12.5 mm) on a micro-strain tester (TA Instruments, USA). The hydrogel was immersed in deionized water through the whole test, as illustrated on Fig. 2a. The stress-relaxation tests were carried out over 20 hours with an instantaneous step strain of 5%.

The migration of water in the hydrogel gives the poroelasticity, while the rearrangements of ionic crosslinks of alginate give the viscoelasticity of the hydrogel [25]. Typical values for the effective diffusivity of water in polyacrylamide hydrogel is $\sim 10^{-9}\,\mathrm{m^2/s}$, and the viscoelastic characteristic time of ionically cross-linked alginate is $\sim 10\,\mathrm{s}$ [25]. Therefore, the material length scale $\sqrt{D\tau}$ can be evaluated to be on the order of 100 μm. Following the large-sample case, we set the radii of the gel disks to vary from 3.675 mm to 7.95 mm, expecting that the sample lengths will be much larger than the material lengths.

Figure 5a shows that the curves of F/a^2 vs. t are initially independent of the radii of the gel disks in a time period $\sim 100\,\mathrm{s}$, where $F \geqslant F_m$. As F decreases below F_m, the curves for gel disks with different radii separate in a longer time period, $10^4 \sim 10^5\,\mathrm{s}$ (Fig. 5a). However, as the time is normalized with the sample size, the curves of F/a^2 vs. t/a^2
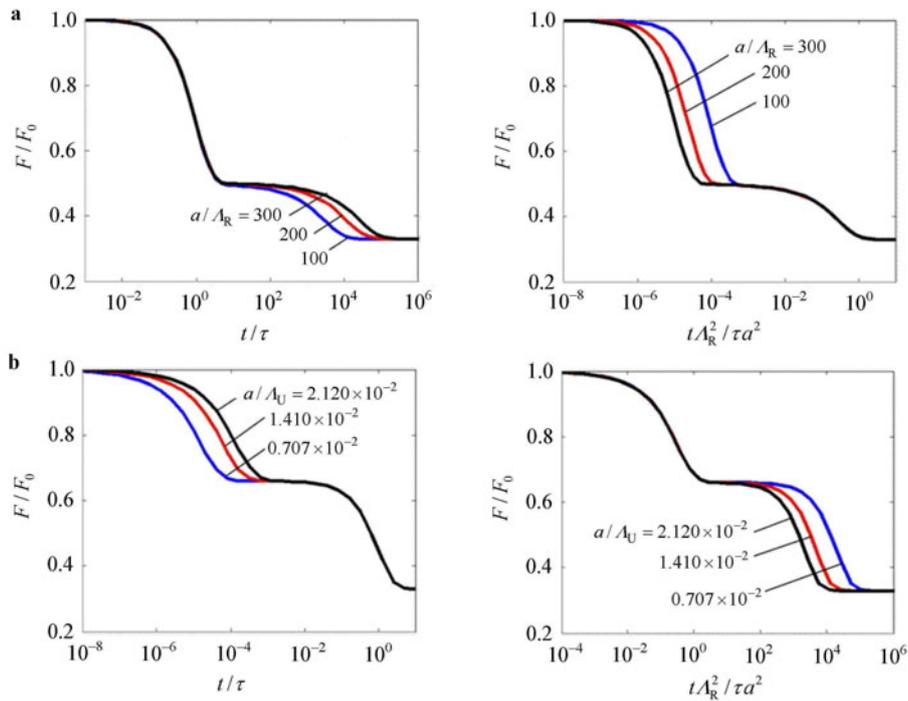
Fig. 4 Results from finite-element models of parallel-plate stress-relaxation tests on a poroviscoelastic gel. **a** The large-sample case; **b** The small-sample case
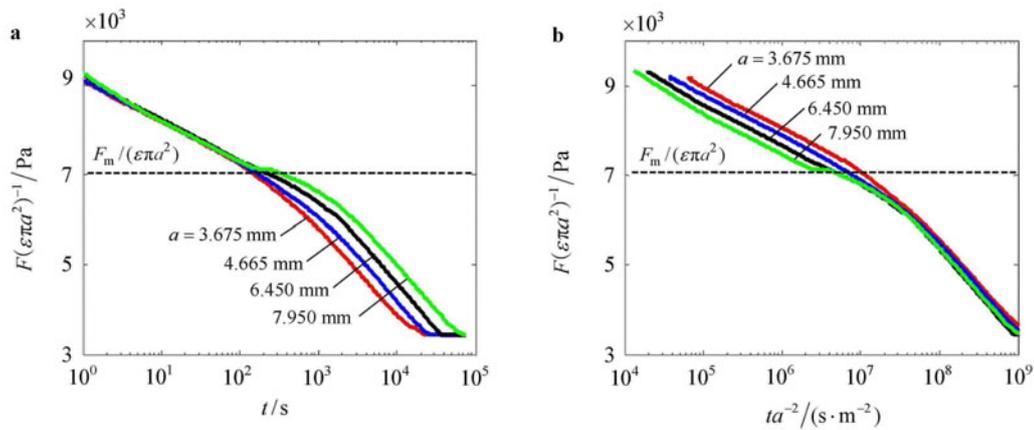
Fig. 5 Parallel-plate stress-relaxation tests on a polyacrylamide-alginate hydrogel in the large-sample case. The stress-relaxation curves of **a** $F/(\varepsilon\pi a^2)$ vs. t and **b** $F/(\varepsilon\pi a^2)$ vs. t/a^2

collapse onto one curve in the region of $F < F_{\mathrm{m}}$ (Fig. 5b). These results validate that the viscoelasticity and poroelasticity of a gel can manifest themselves at different time scales of a test, by setting the sample lengths to be much larger than the material lengths. In addition, the poroviscoelastic parameters of the gel can be obtained in the short-time period through

$$G_{\mathrm{U}} = F_0/(3\pi a^2 \varepsilon), \tag{24a}$$

$$G_{\mathrm{R}} = F_{\mathrm{m}}/(3\pi a^2 \varepsilon), \tag{24b}$$

$$(F - F_{\mathrm{m}})/(F_0 - F_{\mathrm{m}}) = \exp(-t/\tau), \tag{24c}$$

and in the long-time period through

$$v = 3F_\infty/(2F_{\mathrm{m}}) - 1, \tag{24d}$$

$$(F - F_\infty)/(F_{\mathrm{m}} - F_\infty) = f(v, D_{\mathrm{R}} t/a^2), \tag{24e}$$

where F_0 is the instantaneous force, F_∞ is the long-term force, ε is the applied strain, and f is a complicated function given in Ref. [27]. Using Eq. (24), we obtain $G_{\mathrm{U}} = 3.082\,\mathrm{kPa}$, $G_{\mathrm{R}} = 2.42\,\mathrm{kPa}$, $v = -0.278$, $\tau = 15\,\mathrm{s}$, and $D_{\mathrm{R}} = 2.07 \times 10^{-9}\,\mathrm{m}^2/\mathrm{s}$. These values are in the same ranges as the ones from previous tests on viscoelastic and poroelastic properties of gels [25, 27, 32, 44, 45, 61].

5 Conclusions

In summary, we develop a method that can separate the poroelasticity and viscoelasticity of gels at different time scales by setting the sample lengths to be much larger or smaller than the material lengths of the gels. We formulate a theory of ideal linear poroviscoelastic gel and implement it into finite-element models. The finite-element calculations validate our method in separating the viscoelasticity and poroelasticity of gels at different time scales. The validity of this method is further proved with parallel-plate stress-relaxation experiments on a hydrogel in large-sample case. We expect the method can be readily implemented into various tests to probe the properties of poroviscoelastic gels. In particular, gels with physical cross-links [33, 61–64] tend to be poroviscoplastic with $G_R \approx 0$. For poroviscoplastic gels, one needs to adopt the small-sample case, where micro/nano-indentations are particularly useful [29, 32].

References

1 Zwieniecki, M.A., Melcher, P.J., Holbrook, N.M.: Hydrogel control of xylem hydraulic resistance in plants. Science **291**, 1059–1062 (2001)

2 Mow, V.C., Kuei, S.C., Lai, W.M., et al.: Biphasic creep and stress-relaxation of articular-cartilage in compression—heory and experiments. J. Biomech. Eng.-Trans. ASME **102**, 73–84 (1980)

3 Liu, Z., Swaddiwudhipong, S., Hong, W.: Pattern formation in plants via instability theory of hydrogels. Soft Matter **9**, 577–587 (2013)

4 Liu, Z., Hong, W., Suo, Z., et al.: Modeling and simulation of buckling of polymeric membrane thin film gel. Computational Materials Science **49**, S60–S64 (2010)

5 Zhao, X., Kim, J., Cezar, C.A., et al.: Active scaffolds for on-demand drug and cell delivery. Proceedings of the National Academy of Sciences of the United States of America **108**, 67–72 (2011)

6 Lee, K.Y., Mooney, D.J.: Hydrogels for tissue engineering. Chemical Reviews **101**, 1869–1879 (2001)

7 Luo, Y., Shoichet, M.S.: A photolabile hydrogel for guided three-dimensional cell growth and migration. Nature materials **3**, 249–253 (2004)

8 Richter, A., Paschew, G., Klatt, S., et al.: Review on hydrogel-based pH sensors and microsensors. Sensors **8**, 561–581 (2008)

9 Gerlach, G., Guenther, M., Sorber, J., et al.: Chemical and pH sensors based on the swelling behavior of hydrogels. Sensors and Actuators B: Chemical **111**, 555–561 (2005)

10 Suo, Z.: Theory of dielectric elastomers. Acta Mechanica Sol-ida Sinica **23**, 549–578 (2010)

11 Beebe, D.J., Moore, J.S., Bauer, J.M., et al.: Functional hydrogel structures for autonomous flow control inside microfluidic channels. Nature **404**, 588–590 (2000)

12 He, T., Li, M., Zhou, J.: Modeling deformation and contacts of pH sensitive hydrogels for microfluidic flow control. Soft Matter **8**, 3083–3089 (2012)

13 Cai, S., Lou, Y., Ganguly, P., et al.: Force generated by a swelling elastomer subject to constraint. Journal of Applied Physics **107**, 103535 (2010)

14 Barbut, S., Foegeding, E.A.: Ca2+-Induced gelation of pre-heated whey-protein isolate. J. Food Sci. **58**, 867–871 (1993)

15 Hong, W., Zhao, X., Zhou, J., et al.: A theory of coupled diffusion and large deformation in polymeric gels. Journal of the Mechanics and Physics of Solids **56**, 1779–1793 (2008)

16 Yoon, J., Cai, S., Suo, Z., et al.: Poroelastic swelling kinetics of thin hydrogel layers: Comparison of theory and experiment. Soft Matter **6**, 6004–6012 (2010)

17 Li, Y., Tanaka, T.: Kinetics of swelling and shrinking of gels. The Journal of Chemical Physics **92**, 1365–1371 (1990)

18 Quesada-Péez, M., Maroto-Centeno, J.A., Forcada, J., et al.: Gel swelling theories: The classical formalism and recent approaches. Soft Matter **7**, 10536–10547 (2011)

19 Cai, S., Suo, Z.: Equations of state for ideal elastomeric gels. EPL (Europhysics Letters) **97**, 34009 (2012)

20 Hong, W., Liu, Z., Suo, Z.: Inhomogeneous swelling of a gel in equilibrium with a solvent and mechanical load. International Journal of Solids and Structures **46**, 3282–3289 (2009)

21 Kang, M.K., Huang, R.: A variational approach and finite element implementation for swelling of polymeric hydrogels under geometric constraints. Journal of Applied Mechanics **77**, 061004 (2010)

22 Zhang, J., Zhao, X., Suo, Z., et al.: A finite element method for transient analysis of concurrent large deformation and mass transport in gels. Journal of Applied Physics **105**, 093522 (2009)

23 Zhou, J., Huang, G., Li, M., et al.: Stress evolution in a phase-separating polymeric gel. Modelling and Simulation in Materials Science and Engineering **18**, 025002 (2010)

24 Ferry, J.D.: Viscoelastic Properties of Polymers. John Wiley & Sons, Inc., New York (1980)

25 Zhao, X., Huebsch, N., Mooney, D.J., et al.: Stress-relaxation behavior in gels with ionic and covalent crosslinks. Journal of Applied Physics **107**, 063509 (2010)

26 Chen, D.T., Wen, Q., Janmey, P.A., et al.: Rheology of soft materials. Annual Review of Condensed Matter Physics **1**, 301–322 (2010)

27 Cai, S., Hu, Y., Zhao, X., et al.: Poroelasticity of a covalently crosslinked alginate hydrogel under compression. Journal of Applied Physics **108**, 113514 (2010)

28 Hu, Y., Chan, E.P., Vlassak, J.J., et al.: Poroelastic relaxation indentation of thin layers of gels. Journal of Applied Physics **110**, 086103 (2011)

29 Hu, Y., You, J.O., Auguste, D.T., et al.: Indentation: A simple, nondestructive method for characterizing the mechanical and transport properties of pH-sensitive hydrogels. J. Mater. Res. **27**, 152–160 (2012)

30 Hu, Y., Chen, X., Whitesides, G.M., et al.: Indentation of poly-dimethylsiloxane submerged in organic solvents. J. Mater. Res. **26**, 785–795 (2011)

31 Kalcioglu, Z.I., Mahmoodian, R., Hu, Y., et al.: From macro-to microscale poroelastic characterization of polymeric hydrogels via indentation. Soft Matter **8**, 3393–3398 (2012)

32 Strange, D.G., Fletcher, T.L., Tonsomboon, K., et al.: Separating poroviscoelastic deformation mechanisms in hydrogels. Appl. Phys. Lett. **102**, 031913 (2013)

33 Hyland, L.L., Taraban, M.B., Feng, Y., et al.: Viscoelastic properties and nanoscale structures of composite oligopeptide-polysaccharide hydrogels. Biopolymers **97**, 177–188 (2012)

34 Olberding, J.E., Francis Suh, J.: A dual optimization method for the material parameter identification of a biphasic poro-viscoelastic hydrogel: Potential application to hypercompliant soft tissues. J. Biomech. **39**, 2468–2475 (2006)

35 Cheng, L., Xia, X., Scriven, L.E., et al.: Spherical-tip indentation of viscoelastic material. Mech. Mater. **37**, 213–226 (2005)

36 Constantinides, G., Kalcioglu, Z.I., McFarland, M., et al.: Probing mechanical properties of fully hydrated gels and biological tissues. J. Biomech. **41**, 3285–3289 (2008)

37 Ebenstein, D.M., Pruitt, L.A.: Nanoindentation of soft hydrated materials for application to vascular tissues. J. Biomed. Mater. Res. Part A **69A**, 222–232 (2004)

38 Galli, M., Oyen, M.L.: Fast identification of poroelastic parameters from indentation tests. CMES-Comp. Model. Eng. Sci. **48**, 241–269 (2009)

39 Hui, C.Y., Muralidharan, V.: Gel mechanics: A comparison of the theories of Biot and Tanaka, Hocker, and Benedek. J. Chem. Phys. **123**, 154905 (2005)

40 Kaufman, J.D., Miller, G.J., Morgan, E.F., et al.: Time-dependent mechanical characterization of poly(2-hydroxyethyl methacrylate) hydrogels using nanoindentation and unconfined compression. J. Mater. Res. **23**, 1472–1481 (2008)

41 Lin, Y.Y., Hu, B.W.: Load relaxation of a flat rigid circular indenter on a gel half space. J. Non-Cryst. Solids **352**, 4034–4040 (2006)

42 Oyen, M.L.: Poroelastic nanoindentation responses of hydrated bone. J. Mater. Res. **23**, 1307–1314 (2008)

43 Hui, C.Y., Lin, Y.Y., Chuang, F.C., et al.: A contact mechanics method for characterizing the elastic properties and permeability of gels. J. Polym. Sci. Pt. B-Polym. Phys. **44**, 359–370 (2006)

44 Hu, Y.H., Zhao, X.H., Vlassak, J.J., et al.: Using indentation to characterize the poroelasticity of gels. Appl. Phys. Lett. **96**, 121904 (2010)

45 Galli, M., Comley, K.S.C., Shean, T.A.V., et al.: Viscoelastic and poroelastic mechanical characterization of hydrated gels. J. Mater. Res. **24**, 973–979 (2009)

46 Galli, M., Fornasiere, E., Cugnoni, J., et al.: Poroviscoelastic characterization of particle-reinforced gelatin gels using indentation and homogenization. Journal of the Mechanical Behavior of Biomedical Materials **4**, 610–617 (2011)

47 Chiravarambath, S., Simha, N.K., Namani, R., et al.: Poro-viscoelastic cartilage properties in the mouse from indentation. Journal of biomechanical engineering **131**, 011004 (2009)

48 Li, J., Hu, Y., Vlassak, J.J., et al.: Experimental determination of equations of state for ideal elastomeric gels. Soft Matter **8**, 8121–8128 (2012)

49 Liu, Y., Chan-Park, M.B.: Hydrogel based on interpenetrating polymer networks of dextran and gelatin for vascular tissue engineering. Biomaterials **30**, 196–207 (2009)

50 Hui, C., Feng, X., Jagota, A.: In situ measurement of the viscoelastic modulus of gels using pure twist-theory. Soft Matter **9**, 913–920 (2013)

51 Wang, X., Hong, W.: A visco-poroelastic theory for polymeric gels. Proceedings of the Royal Society A: Mathematical, Physical and Engineering Science **468**, 3824–3841 (2012)

52 Hu, Y., Suo, Z.: Viscoelasticity and poroelasticity in elastomeric gels. Acta Mechanica Solida Sinica **25**, 441–458 (2012)

53 Biot, M.: Theory of deformation of a porous viscoelastic anisotropic solid. Journal of Applied Physics **27**, 459–467 (1956)

54 Weitsman, Y.: Stress assisted diffusion in elastic and viscoelastic materials. Journal of the Mechanics and Physics of Solids **35**, 73–94 (1987)

55 Weitsman, Y.: A continuum diffusion model for viscoelastic materials. Journal of Physical Chemistry **94**, 961–968 (1990)

56 Govindjee, S., Simo, J.C.: Coupled stress-diffusion: Case II. Journal of the Mechanics and Physics of Solids **41**, 863–887 (1993)

57 McBride, A.T., Bargmann, S., Steinmann, P.: Geometrically nonlinear continuum thermomechanics coupled to diffusion: a framework for case II diffusion. Advances in Extended and Multifield Theories for Continua. Springer, 89–107 (2011)

58 Gong, J.P., Katsuyama, Y., Kurokawa, T., et al.: Double-network hydrogels with extremely high mechanical strength. Advanced Materials **15**, 1155–1158 (2003)

59 Zhao, X.H.: A theory for large deformation and damage of interpenetrating polymer networks. Journal of the Mechanics and Physics of Solids **60**, 319–332 (2012)

60 Wang, X., Hong, W.: Pseudo-elasticity of a double network gel. Soft Matter **7**, 8576–8581 (2011)

61 Sun, J.Y., Zhao, X., Illeperuma, W.R., et al.: Highly stretchable and tough hydrogels. Nature **489**, 133–136 (2012)

62 An, Y., Solis, F.J., Jiang, H.: A thermodynamic model of physical gels. Journal of the Mechanics and Physics of Solids **58**, 2083–2099 (2010)

63 Henderson, K.J., Zhou, T.C., Otim, K.J., et al.: Ionically cross-linked triblock copolymer hydrogels with high strength. Macromolecules **43**, 6193–6201 (2010)

64 Hui, C.Y., Long, R.: A constitutive model for the large deformation of a self-healing gel. Soft Matter **8**, 8209–8216 (2012)